

## Continued Fractions Hierarchy of Rotation Numbers in Planar Dynamics

Carl Robert,<sup>1,\*</sup> Kathleen T. Alligood,<sup>2</sup> and Timothy D. Sauer<sup>2</sup>

<sup>1</sup>*Institute for Plasma Research and Department of Physics, University of Maryland, College Park, Maryland 20742*

<sup>2</sup>*Department of Mathematical Sciences, George Mason University, Fairfax, Virginia 22030*

(Received 10 June 1999)

Global bifurcations such as crises of attractors, explosions of chaotic saddles, and metamorphoses of basin boundaries play a crucial role in understanding the dynamical evolution of physical systems. Global bifurcations in dissipative planar maps are typically caused by collisions of invariant manifolds of periodic orbits, whose dynamical behaviors are described by rotation numbers. We show that the rotation numbers of the periodic orbits created at certain important tangencies are determined by the continued fraction expansion of the rotation number of the orbit involved in the collision.

PACS numbers: 05.45.Ac, 02.10.Lh, 05.45.Pq, 06.30.Gv

In complex experimental systems, nonlinearities trigger sudden changes in system behavior which are not caused by local bifurcations. Much attention has focused on crises of attractors [1], metamorphoses of basin boundaries [2], and more recently on explosions of chaotic saddles [3,4]. It has been established that these global bifurcations are typically triggered by collisions of certain invariant manifolds associated with particular periodic orbits. At such a collision, the complication of the dynamics changes markedly, as infinitely many other periodic orbits are created. Particularly important for planar systems is the rotation number of the orbit, which measures average rotation around the chaotic invariant set in question [5]. Comprehensive studies of rotation numbers in two-dimensional phase spaces include those of dissipative twist maps [6] and one-parameter families of invertible planar maps [7]. In this Letter we report on a simple method to express the periods, and more generally the rotation numbers, of the infinity of periodic orbits that are born at these global bifurcations. The new rotation numbers can be expressed in terms of a continued fraction expansion of the orbit involved in the bifurcation. Moreover, the hierarchy of the periodic orbits formed corresponds exactly to the “depth” of the rotation number when written in its continued fraction expansion.

Continued fractions are useful in several different scientific disciplines, often where approximation of irrational numbers is required. They are used for renormalization group theory [8], to estimate the eigenvalues of the Frobenius-Perron operator [9], to approximate irrational winding numbers for Kol'mogorov-Arnol'd-Moser tori [10] and the critical parameter values at which these tori break [11], and to obtain minimizing periodic orbits [12]. They are used in an algorithm for computing stable and unstable directions of maps [13]. There is also a so-called matrix continued fraction expansion technique that can be applied to a model for Bloch electrons in a magnetic field [14] and to the Fokker-Planck equation [14,15]. They are also used to describe winding numbers in diode resonator systems [16].

Figure 1 shows rotation numbers for accessible periodic orbits on a chaotic attractor  $A_\mu$  for the Hénon map

$$(x, y) \rightarrow (\mu - x^2 - 0.3y, x), \quad (1)$$

where  $\mu$  is a scalar parameter. A point  $z$  on the attractor is called *accessible* if there is a path in the complement of  $A_\mu$  which has  $z$  as its only limit point in  $A_\mu$ . For a fixed parameter value all accessible orbits rotate around the edge of the attractor at the same asymptotic rate [17]. The devil's staircase structure of this graph reflects the order in which periodic orbits are incorporated into the Hénon attractor as the accessible periodic orbits. We examine how and with what rotational structure these orbits are created.

We begin by illustrating the birth of periodic orbits at a rotary tangency. Figure 2(a) shows a sketch of a period-3 orbit undergoing a  $p_1 \rightarrow p_2 \rightarrow p_3 \rightarrow p_1$  rotation. Also drawn are the stable manifolds and the interior branches of the unstable manifolds of the three points. The interior

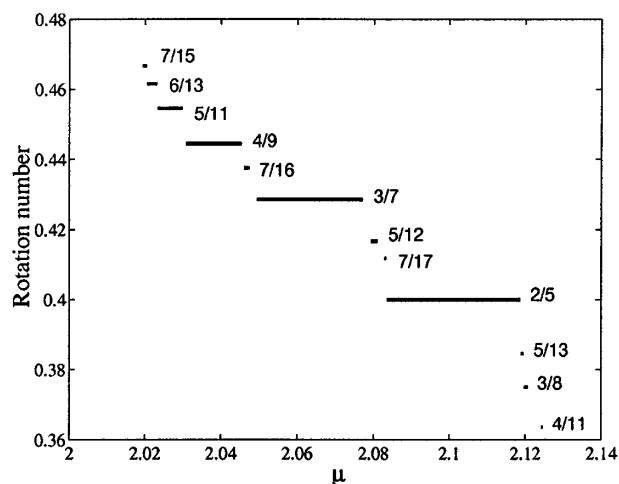


FIG. 1. Devil's staircase of accessible rotation numbers for the Hénon map, Eq. (1). The graph shows the rotation rate of the periodic orbits on the outside edge of the attractor as a function of the parameter  $\mu$ . Although there are periodic orbits of infinitely many periods in the attractor, all accessible points rotate around the outside edge of the attractor at an identical rate.

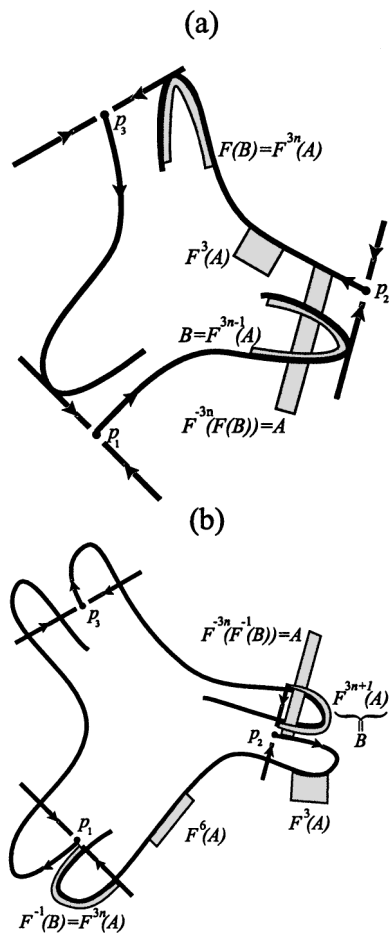


FIG. 2. Sketches of rotary tangencies. (a) At a co-rotary inner tangency. The box denoted  $A$  has horseshoe dynamics under the  $(3n - 1)$ th iterate of the map  $F$ . (b) Slightly after a counter-rotary outer tangency. The box denoted  $A$  forms a horseshoe under the  $(3n + 1)$ th iterate of the map.

branch of the unstable manifold of a point  $p_n$  in the orbit is tangent to a branch of the stable manifold of the next point in the orbit  $p_{n+1}$ . These simultaneous tangencies produce a simple closed curve, formed by alternating pieces of unstable and stable manifolds, which goes through all points in the periodic orbit. This type of tangency, when an unstable manifold collides with the stable manifold of an adjacent point of the same periodic orbit, is called a *rotary tangency* [18,19].

The two-dimensionality of the plane restricts rotary tangencies to two distinct types. The two types of rotary tangency are distinguished by whether the unstable manifold participating in the tangency travels in the direction of rotation of the periodic orbit, or against that direction. In terms of Fig. 2(a), the two possibilities are (i) the unstable manifold of  $p_n$  is tangent to the stable manifold of  $p_{n+1}$  or (ii) the unstable manifold of  $p_n$  is tangent to the stable manifold of  $p_{n-1}$ . We call the former a *co-rotary tangency* since the unstable manifold turns toward the next point in the rotational order; the latter is called a *counter-rotary tangency* since the unstable manifold turns to the previous point in the rotational order. At a rotary tangency of a

periodic orbit with a general rational rotation number, the unstable manifold always turns toward an adjacent point in the orbit, which is not necessarily the next or previous iterate.

For example, for a period-7 orbit of rotation number  $2/7$ , the order of the points in the orbit along a circle would be  $p_1 \rightarrow p_5 \rightarrow p_2 \rightarrow p_6 \rightarrow p_3 \rightarrow p_7 \rightarrow p_4 \rightarrow p_1$ . In this case, the unstable manifold of  $p_1$  is tangent to the stable manifold of  $p_5$  in the co-rotary case and to the stable manifold of  $p_4$  in the counter-rotary case.

There is a second distinction to be made among rotary tangencies: the branch of the unstable manifold can be tangent so as to limit on the corresponding unstable branch of the adjacent point in the orbit—or it can limit on the opposite branch at the adjacent point. The first is called an *inner tangency*, while the second is called an *outer tangency*. Figure 2(a) depicts an inner tangency, and Fig. 2(b) shows an outer tangency. In this figure, the inner tangency is co-rotary, and the outer tangency is counter-rotary. At an inner rotary tangency, periodic orbits are created inside the closed curve formed by the tangent manifolds. For area-contracting maps, such as maps in the Hénon family, these periodic orbits are all created before the tangency.

Let  $F$  be an invertible planar map. In order to calculate the periods of orbits of  $F$  created at an inner tangency, we analyze the formation of horseshoes [20], as depicted in Fig. 2(a). Begin with the horseshoe-shaped region marked  $B$ . Iterate forward to  $F(B)$ , and consider backward images of  $F(B)$  along the unstable manifold of  $p_2$ . (Every third iterate of  $F^{-1}$  moves the region back along the unstable manifold toward  $p_2$ .) For some  $n$ ,  $F^{-3n}(F(B))$  reintersects  $B$ . Let  $A = F^{-3n}(F(B)) = F^{-3n+1}(B)$ . Thus  $F^{3n-1}$  maps the rectangle  $A$  over itself in a horseshoe image. The invariant set of this horseshoe has periodic orbits which are multiples of the minimum period  $3n - 1$ . For each  $n$  sufficiently large, such a horseshoe is formed. (See [19] for details of the construction.) We concentrate on the regular saddle of (minimum) period  $3n - 1$  in each horse-shoe [21].

We can also calculate the rotation number of these saddles, the rotation being calculated along the closed curve formed by the rotary tangency. In the  $3n - 1$  iterates it takes for the horseshoe image to reintersect the rectangle, the region has completed  $n$  rotations near the closed curve, and thus the saddle has rotation number  $n/(3n - 1)$ . These orbits exist at least for  $n$  sufficiently large, and, in particular, there are infinitely many of them. To express these rotation numbers as continued fractions, denote

$$[a_1, a_2, \dots, a_j] = \frac{1}{a_1 - \frac{1}{a_2 - \frac{1}{a_3 - \dots - \frac{1}{a_j}}}}, \quad (2)$$

where the  $a_i$  are positive integers, and the integer  $j$  is called the *depth* of the expansion. Figure 2(a) shows a co-rotary inner tangency of a period-3 orbit with rotation number  $[3] = 1/3$ . The new rotation numbers created at this tangency are of form  $[3, n] = n/(3n - 1)$ . More generally, the following fact [19] holds.

*Fact 1.* At a co-rotary tangency of a periodic orbit with rotation number  $[a_1, \dots, a_j]$  as in Eq. (2), infinitely many periodic orbits are created with rotation numbers  $[a_1, \dots, a_j, n]$  for all sufficiently large  $n$ .

Figure 3(a) shows a computer study of a period-3 co-rotary inner tangency of the Hénon map, occurring at  $\mu \approx 2.12468$ . Only part of the manifolds have been computed to be able to distinguish the points of tangency. This event leads to a boundary crisis [23]. The  $3/8 = [3, 3]$  saddle first appears at  $\mu \approx 1.99531$ , while the  $4/11 = [3, 4]$  saddle is created at  $\mu \approx 2.11319$ . Thus the tangency of the invariant manifolds of the depth 1 orbits leads to the creation of infinitely many depth 2 orbits, each of which leads to depth 3 orbits and so on. The continued fraction depth provides an organizational hierarchy for these periodic orbits.

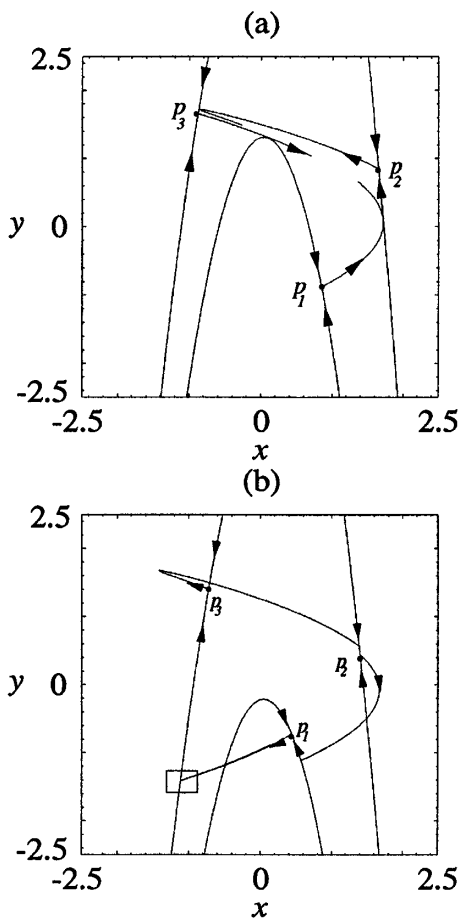


FIG. 3. Rotary tangencies for the Hénon map. (a) Inner tangency at  $\mu_c \approx 2.12468$  (triggers a boundary crisis). (b) Outer tangency at  $\mu \approx 1.38031$  (triggers an isolated chaotic saddle explosion). The rectangle shows the location of one of the tangency points. The computer simulations of Figs. 3 and 4 used DYNAMICS [22].

The pattern of rotation numbers which arise at a counter-rotary tangency is given by a slightly different type of continued fraction. Figure 2(b) shows a counter-rotary outer tangency of a period-3 orbit. A rectangular domain maps back over itself after  $3n + 1$  iterates. These periods are observed in [3]. In this case, there is a sequence of saddles, one of each rotation number  $n/(3n + 1)$ , for  $n$  sufficiently large, converging to points in the period-3 orbit. Note that in this case, horseshoes can form only outside the closed curve formed by the tangent manifolds. For an area-contracting map, they form only after the tangency has occurred, as shown in Fig. 2(b).

For the counter-rotary tangency, we need to introduce the continued fraction

$$\{a_1, a_2, \dots, a_j\} = \frac{1}{a_1 + \frac{1}{a_2 - \frac{1}{a_3 - \dots - \frac{1}{a_j}}}} \quad (3)$$

In the example above, the counter-rotary tangency of the period-3 orbit creates a sequence of saddles, one of each rotation number  $\{3, n\} = n/(3n + 1)$ , for sufficiently large  $n$ . More generally, the following holds.

*Fact 2.* At a counter-rotary tangency of a periodic orbit with rotation number  $\{a_1, \dots, a_j\}$  as in Eq. (3), infinitely many periodic orbits are created with rotation numbers  $\{a_1, \dots, a_j, n\}$  for all sufficiently large  $n$ .

Figure 3(b) shows a counter-rotary outer tangency of a period-3 saddle of the Hénon map. At this tangency, periodic orbits with rotation numbers  $\{3, n\} = n/(3n + 1)$  are formed, for  $n \geq 2$ . A  $2/7 = \{3, 2\}$  orbit (shown in Fig. 4) for this family of maps has a counter-rotary outer tangency at approximately  $\mu = 1.385$  that creates orbits with rotation numbers  $\{3, 2, n\} = (2n - 1)/(7n - 3) = [2(n - 1) + 1]/[7(n - 1) + 4]$ , for all sufficiently large  $n$ .

Facts 1 and 2 follow from the above discussion and elementary properties of continued fractions. In the co-rotary case (Fact 1), consider an orbit with rotation number  $M/N = [a_1, \dots, a_j]$ . Assume that the box  $A$  in Fig. 2(a) is moved after  $(n - 1)N$  iterations of the map along the unstable manifold until it maps in the vicinity of the adjacent orbit point in the direction of the orbit rotation. During this time it will have made slightly more than  $(n - 1)M$  rotations. From this point, the number of iterations required to map the box back over itself is  $K$ , where  $H/K = [a_1, \dots, a_j - 1]$ . This follows from the fact that  $H/K$  is the unique solution of the equation  $1 + KM = 0 + HN$ , up to multiples of  $N$ . Since  $H$  extra rotations will have occurred, the rotation number of the new orbit created as in Fig. 2(a) will be  $[(n - 1)M + H]/[(n - 1)N + K] = (n - 1)[a_1, \dots, a_j] \oplus [a_1, \dots, a_j - 1] = [a_1, \dots, a_j, n]$ , where  $\oplus$  denotes Farey sum. The proof of Fact 2 is analogous, although the box precesses opposite to the direction of rotation during

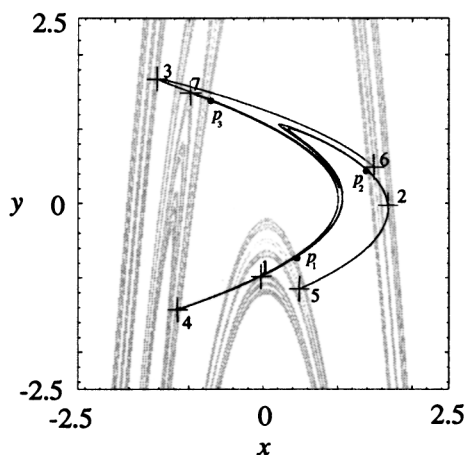


FIG. 4. A period-3 orbit  $p_1, p_2, p_3$  with its stable (grey) and unstable (black) manifolds computed slightly after counter-rotary outer tangency ( $\mu \approx 1.38477$ ). Also shown is a period-7 orbit (rotation number  $2/7$ ) which has been created after the outer tangency of the period-3 orbit. Notice that the period-7 orbit is in the neighborhood of the tangency points.

the  $(n-1)N$  iterations. In this case we must define  $M/N = \{a_1, \dots, a_j\}$  and  $H/K = \{a_1, \dots, a_j - 1\}$ , because they solve the equation  $-1 + KM = 0 + HN$ , and so the rotation number of the new orbit will be  $[(n-1)M + H]/[(n-1)N + K] = \{a_1, \dots, a_j, n\}$ .

In the Hénon family there are infinitely many inner and outer rotary tangencies. (In [19] it is shown that an inner rotary tangency at one level implies the existence of infinitely many rotary tangencies at the next level.) The fact that the inner tangencies are co-rotary and the outer tangencies are counter-rotary follows from the relative speeds of the rotations on either side of the mediating periodic orbit (i.e., the orbit that undergoes the tangency). In Fig. 3 there is a fixed point in the lower left of the picture (not shown). Points move more slowly outside the period three orbit than inside, due to the presence of the fixed point. Thus the unstable manifolds turn in the opposite direction to the rotation of the map (counter-rotary) for the outer tangency, and in the same direction (co-rotary) for the inner tangency. There is no reason to assume that the designations of co-/counter-rotary and inner/outer tangency are dependent, although the circumstance that links them in the Hénon map would seem to be a typical one.

Figure 1 hints at the complexity of rotation numbers created by the process described above. The accessible orbits undergo rotary tangencies, creating an infinite sequence of periodic orbits, each of which repeats the process on a finer scale. The continued fraction representation of rotation numbers provides a simple hierarchical description of this complex web of periodic orbits.

C. R. was supported in part by the FCAR (Fonds pour la Formation de Chercheurs et l'aide à la Recherche). C. R. thanks M. Dutta for his helpful comments. The research of T.S. was partially supported by the Computational Mathematics program of the NSF.

\*Current address: Department of Physics, University of California, Santa Barbara, CA 93106.

- [1] C. Grebogi, E. Ott, and J. A. Yorke, Phys. Rev. Lett. **48**, 1507 (1982); Physica (Amsterdam) **7D**, 181 (1983).
- [2] The term metamorphosis has been used to denote a sudden jump in the basin boundary. C. Grebogi, E. Ott, and J. A. Yorke, Phys. Rev. Lett. **56**, 1011 (1986); Physica (Amsterdam) **24D**, 243 (1987); S. M. Hammel and C. K. R. T. Jones, Physica (Amsterdam) **35D**, 87 (1989); K. T. Alligood, L. Tedeschini-Lalli, and J. A. Yorke, Commun. Math. Phys. **120**, 105 (1991).
- [3] C. Robert, K. T. Alligood, E. Ott, and J. A. Yorke, Phys. Rev. Lett. **80**, 4867 (1998).
- [4] C. Robert, K. T. Alligood, E. Ott, and J. A. Yorke, Physica D (Amsterdam) (to be published).
- [5] For an invertible circle map  $f$ , a periodic orbit of  $f$  has rotation number  $p/q$  (in reduced form) if the period of the orbit is  $q$  and if the orbit goes around the circle  $p$  times every  $q$  iterates.
- [6] M. Casdagli, Ergod. Theory Dyn. Syst. **7**, 165 (1987).
- [7] M. Barge, in *Continuum Theory and Dynamical Systems*, edited by T. West (Marcel Dekker, New York, 1993), p. 15.
- [8] W. Gautschi, SIAM J. Numer. Anal. **7**, 187 (1970); P. Henrici, in *Applied and Computational Complex Analysis* (Wiley, New York, 1977), Vol. 2; W. B. Jones and W. J. Thron, in *Continued Fractions: Analytic Theory and Applications* (Addison-Wesley, Reading, 1980); S.-h. Kim and S. Ostlund, Phys. Rev. Lett. **55**, 1165 (1985).
- [9] H. Fujisaka and M. Inoue, Prog. Theor. Phys. **78**, 1203 (1987); Phys. Rev. A **39**, 4778 (1989); H. Fujisaka, H. Shigematsu, and B. Eckhardt, Z. Phys. B **92**, 235 (1993).
- [10] J. D. Meiss, Phys. Rev. A **34**, 2375 (1986); M. Z. Fuka *et al.*, Phys. Rev. E **51**, 1935 (1995).
- [11] J.-m. Mao and R. H. G. Helleman, Phys. Rev. A **39**, 344 (1989).
- [12] H. J. Schellnhuber and H. Urbschat, Phys. Rev. A **38**, 5888 (1988).
- [13] M. Paramio and J. Sesma, Phys. Lett. A **132**, 98 (1998).
- [14] G. Petschel and T. Geisel, Phys. Rev. Lett. **71**, 239 (1993).
- [15] R. Walser *et al.*, Phys. Rev. A **45**, 468 (1992).
- [16] Z. Su, R. W. Rollins, and E. R. Hunt, Phys. Rev. A **36**, 3515 (1987); Phys. Rev. A **40**, 2689 (1989).
- [17] K. T. Alligood and J. A. Yorke, Ergod. Theory Dyn. Syst. **12**, 377 (1992).
- [18] K. Hockett and P. Holmes, Ergod. Theory Dyn. Syst. **6**, 205 (1986).
- [19] K. T. Alligood and T. D. Sauer, Commun. Math. Phys. **120**, 105 (1988).
- [20] K. T. Alligood, T. D. Sauer, and J. A. Yorke, *Chaos: An Introduction to Dynamical Systems* (Springer-Verlag, New York, 1997).
- [21] A regular saddle of period  $q$  is one in which the Jacobian matrix  $DF^q$  has positive eigenvalues.
- [22] H. E. Nusse and J. A. Yorke, *Dynamics: Numerical Explorations* (Springer-Verlag, New York, 1998), 2nd ed.
- [23] A boundary crisis is defined as a chaotic attractor colliding (while varying a parameter) with its own basin boundary. It leads to the destruction of the attractor.